MODAL ANALYSIS OF MULTI-REFERENCE IMPACT TEST DATA FOR STEEL STRINGER BRIDGES

F.N. Catbas*, M. Lenett*, D.L. Brown*, S.W. Doebling+, C.R. Farrar+, A. Turer*

*University of Cincinnati
Infrastructure Institute
741 Baldwin Hall, ML 71
Cincinnati, OH 45221

+Los Alamos National Laboratory
Engineering Analysis Group
Los Alamos, NM 87454

ABSTRACT. *A comparative study on the post-processing of experimental modal data from a full scale steel stringer bridge for damage identification is presented. The bridge was tested before and after removal of one of the bearing plates at one abutment. Frequency Response Functions, measured at different spatial locations, are used to post-process the data using a Complex Mode Indicator Function(CMIF) algorithm. Dynamic properties of the bridge show major differences between the two cases. In addition, modal flexibility of the bridge is calculated for the measured degrees of freedom. Modal flexibility of the bridge shows good agreement with static instrumentation results under truck loading. The induced damage is successfully quantified for this loading case. The "after-removal" condition data was also post-processed at Los Alamos National Laboratory using the Eigensystem Realization Algorithm (ERA) in order to provide a distant check and correlation for the results. This paper briefly describes the two different algorithms and presents the results in both modal and flexibility space. Further, the principal focus of this paper is the post-processing algorithms and one damage index, although a number of different damage identification indices are being used for varying levels and types of damage as part of the ongoing research project.*

NOMENCLATURE

$[U]$: Matrix of Mass Normalized Mode Shapes

$[f]$: Flexibility Matrix

$[\Omega]$: Inverse of the Diagonal Matrix of Modal Frequencies

$\phi^k(i)$: Modal Vector Coefficient at ith Point for kth Mode

ω_i : Radian Frequency for i - th Mode

X : Response

F : Input Force

$[B(s)]$: System Impedance Matrix

$[H(s)]$: Transfer Function

$[H(\omega)]$: Frequency Response Function

$(A_{pq})_r$: Residue for Resp. Point p, Ref. Point q, of Mode r

λ_r : r - th Complex Eigenvalue or System Pole

$\lambda_r = \sigma_r + j\omega_r$

M_{A_r} : Modal A for rth Mode

ψ_{pr} : Response of Point p for Mode r

$$(A_{pq})_r = \frac{\psi_{pr}\psi_{qr}}{M_{A_r}}$$

1. INTRODUCTION

Experimental study of structural vibration contributes to the understanding and control of structural system behavior. Experimental modal analysis can be described as the process of determining the modal parameters (frequencies, damping factors, modal vectors, and modal scaling) of a linear, time invariant system using an experimental approach. Traditionally, the main objectives for experimental modal analysis were to determine the nature and extent of vibration response levels and to verify and correct theoretical models and predictions [1]. Today, different engineering disciplines use this method for a number of applications. System identification (more specifically, structural identification) based on modal analysis and testing has been successfully utilized by various researchers [2,3].

Structural identification techniques incorporating modal parameters can yield good results for analytical or experimental cases where all external conditions are controlled. For civil engineering structures which

have scattered system characteristics and are subject to changing environmental conditions, both testing and post-processing of the modal data require a modified strategy. Linearity, reciprocity, stationarity and observability, which are the basic assumptions of modal analysis, can be difficult to satisfy for actual civil engineering structures as compared to structural systems under controlled laboratory conditions. The effects that disturb these basic assumptions, and improved testing techniques to counteract these effects, are presented in the experimental counterpart to this paper [4]. Improved post-processing techniques, associated computations, and the results in modal and flexibility spaces, are described in this paper.

In April 1995, researchers from the University of Cincinnati Infrastructure Institute began testing a 3-span steel stringer bridge located in Cincinnati (HAM-561-0683). This bridge, which serves as the research test specimen, is being subjected to a sequence of induced damages. The progress of this research has been presented to a peer review panel consisting of expert researchers from different universities, research institutes, and laboratories. The panel meetings are held intermittently as part of the progress of the research. In this context, it was requested that researchers from Los Alamos National Laboratory analyze and post-process one set of modal data. The two data sets taken before and after the removal of one bearing plate, the analysis and post-processing of this data done at the University of Cincinnati, and the results of the removal case from Los Alamos National Laboratory are discussed.

2. COMPLEX MODE INDICATOR FUNCTION

Multiple Reference Impact Testing(MRIT) was used as a testing procedure, for modal testing of the Seymour bridge (HAM-561-0683). The multiple reference testing procedure measures data from a large number of reference positions, thereby increasing the spatial information in the data set, which is useful for uncoupling closely-spaced modes of the system. However, the type of structures typically tested with MRIT and the conditions under which the testing is conducted often tend to create particular difficulties in extracting reliable modal parameters from the measurements. This is true for the Seymour bridge. In general, on bridge type structures the response of the structure is influenced by ambient conditions. The eigenvalues and eigenvectors vary with temperature and soil conditions. Most of the commercially available multiple reference modal parameter estimation algorithms are based upon consistent data, as a result, using these algorithms it becomes difficult to sort out the computational modes from the system modes. Most of the commercial algorithms, particularly the time domain algorithms, it is necessary to over specify the expected number of algorithms in order to get good fits to the data. In order, to reduce or to eliminate this problem a specialized frequency domain parameter estimation algorithm was developed where it is not necessary to over specify the number of modes.

The method is referred to as the Complex Mode Indicator Function (CMIF). The CMIF method is a spatial domain method where the eigenvectors are estimated directly by using Singular Values Decomposition (SVD) of the measured Frequency Response Function (FRF) matrix. A plot of the Singular Values (SV) of the FRF matrix (CMIF Plot) is used to determine the location and number of eigenvalues in a data set. Peaks in the CMIF plot are locations of the eigenvalues. Tracking the SV's and picking off the peaks is the operator interaction necessary. At the peaks the SV vector (CMIF vector) is the best least squares estimate of the eigenvector for the selected peak. The CMIF vector is used as a spatial filter to compute an Enhanced Frequency Response Function (EFRF) from weighted average of the FRF matrix. The resulting EFRF in the vicinity of the selected peak the EFRF looks like the FRF measured on a Single-Degree-of-Freedom (SDOF) system. A simple SDOF estimation algorithm can be used to estimate the eigenvalue (frequency and damping) and the modal scale factor.

For cases with a large number of references the spatial averaging does an excellent job of isolating each individual eigenvalue-eigenvector pair. A more detailed description of the CMIF can be found in a number of excellent references [5,6,7,8]. As a result, of this study an enhanced CMIF procedure has been developed to handle cases where the EFRF's do not show a SDOF behavior [9].

3. POST-PROCESSING STRATEGY AND QUALITY CONTROL ISSUES

Quality control and post-processing are interrelated, inseparable issues. The quality control measures are explained in detail in the experimental counterpart to this paper. In this paper, the post-processing strategy and basic quality control issues are presented.

The major component of post-processing is the parameter estimation, which is conducted in several stages. First, an estimate of the number of modes in the frequency range of interest is made. CMIF is an appropriate method for use with multi-reference data

which may contain repeated, or nearly repeated, complex modes, as in our case. CMIF can be applied to the entire frequency band of interest or to specific parts of it. Post-processing at UCII is conducted using the X-MODAL Modal Analysis package developed at the University of Cincinnati Structural Dynamics Research Laboratory (UC-SDRL) [10]. The poles can be selected from the screen once the number and location of the poles are identified. After residue calculation, curve-fit plots, and animation of the individual modes, Modal Assurance Criterion (MAC) computations are the quality control of the results in the modal space. Curve-fit plots show how well the measured and the reconstructed model correlate. Animation of the individual modes indicate if any anomaly in the extracted modes exists. Any discontinuous motion or out-of-phase problems can be detected at this stage. The proportional damping/normal mode assumption requires the phase between measurement points to be either 0 or 180 degrees. Visual verification via animation is a good way to check the results of these assumptions. The final quality control step is conducted in the flexibility space. Modal flexibility is calculated from the modal parameters and is loaded with uniform load to check the initial deflected shapes to see whether deflected surface under uniform load is acceptable. Irrelevant deflected shapes are indications of anomalies of the data in the flexibility space due to reasons such as missing modes, computational modes, or bad data. The basic steps in post-processing the experimental data are summarized in Figure 1.

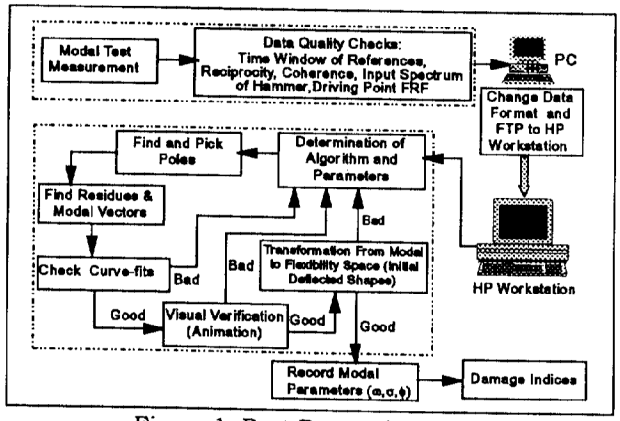

Figure 1: Post-Processing Strategy

4. MODAL FLEXIBILITY COMPUTATION AND ITS APPLICATION TO BRIDGE DATA

The concept of flexibility was first introduced by Maxwell in 1864, and can be described as follows: The displacement influence coefficients comprise the inverse of the flexibility matrix, which is the stiffness matrix of the system. Although most physical structures are continuous, their behavior can usually be represented by a discrete parameter model. The idealized elements that describe this kind of a system are mass, stiffness, and damping of the system. Flexibility, as a system property, has a significant importance to understanding the structural behavior.

Previous researches have shown that modal flexibility can be derived from modal parameters obtained from modal tests. Flexibility has been proposed as a reliable signature reflecting the existing condition of bridges. Flexibility can be derived from the experimental modal data, and can, therefore, be used directly to check the absolute difference between two sets of modal data from two modal tests taken at two different bridge inspection times [3]. The transformation of the natural frequencies and mode shapes to the unit load flexibility matrix is given by the expression:

$$[f_{i,j}] = [U][\Omega][U]^T$$

or can be written more explicitly as:

$$f_{i,j} = \sum_{k=1}^{m} \frac{\phi^k(i)\phi^k(j)}{\omega_k^2}$$

where

$\phi^k(i)$ = the modal vector coefficient at the i-th measurement point of the k-th unit mass-normalized mode vector;

$f_{i,j}$ = the flexibility coefficient at the i-th point under the unit load at point j;

ω_i = the i-th radian frequency (radian/second)

The formulations derived above are based on the unit-mass-normalized vectors. However, the real life structures cannot always be approximated as being proportionally damped. In this paper, a more general computation method is presented which can be applied for real normal modes or complex mode cases. The general mathematical derivation of a multi-degree of freedom system is expressed using Newton's second law as;

$$[M]\{\ddot{x}\}+[C]\{\dot{x}\}+[K]\{x\}=\{f\}$$

The Laplace transform of this equation, assuming all initial conditions are zero, yields:

$$\left[s^2[M]+s[C]+[K]\right]\{X(s)\}=\{F(s)\}$$

Let:

$$[B(s)]=\left[s^2[M]+s[C]+[K]\right]$$

then we can rewrite the above equation as;

$$[B(s)]\{X(s)\}=\{F(s)\}$$

where [B(s)] is referred to as the system impedance matrix or just the system matrix. The transfer matrix can then be formulated as:

$$[B(s)]^{-1}=[H(s)]$$

Then the following equality can be defined:

$$[H(s)]\{F(s)\}=\{X(s)\}$$

The Frequency Response Function is the transfer function evaluated along the frequency axis.

$$[H(s)]_{s=j\omega}=[H(\omega)]$$

Frequency response functions then can be defined from the system characteristics as follows:

$$[-\omega^2[M]+j\omega[C]+[K]]^{-1}=[H(\omega)]$$

A frequency response function can be given in partial fraction form as follows:

$$H_{pq}(\omega)=\sum_{r=1}^{N}\left[\frac{(A_{pq})_r}{j\omega-\lambda_r}+\frac{(A^*_{pq})_r}{j\omega-\lambda^*_r}\right]$$

Modal flexibility matrix can then be computed in terms of the identified modal parameters of the structure evaluated at jw=0 as:

$$H_{pq}(\omega=0)=\sum_{r=1}^{N}\left[\frac{\psi_{pr}\psi_{qr}}{M_{A_r}(-\lambda_r)}+\frac{\psi^*_{pr}\psi^*_{qr}}{M^*_{A_r}(-\lambda^*_r)}\right]$$

The general formulation given above is independent of the normal mode assumption or unit mass normalized vectors. However, this formula is an approximation of a real flexibility matrix because of the truncated number of modes obtainable in practice. Modal truncation effect should be minimized with an appropriate number of identified experimental modes. It is necessary to study the truncation effect of the modal number in the above formula, as the mode number obtained from experiment is always limited. Therefore, the modal truncation effects are investigated under different load cases, and Load Dependent Modal Flexibility Convergence (LMC) plots are generated in order to have a quick check for the truncation effects for the included number of modes. The LMC plots can be defined as follows.

Let us assume m modes are identified from the post-processed data. For m different modes, m different modal flexibility matrices can be obtained, each time adding one higher mode to the flexibility matrix. The deflections at each DOF for a particular load pattern can be computed by loading these m different modal flexibility matrices. Finally, m deflected shapes are obtained for 1,2,...m modes included in the flexibility matrix. The sum of the squares of the differences of deflection values at each degree of freedom is obtained when a new mode is added to the flexibility matrix. Figure 2 shows the convergence of the modal flexibility for an incremental mode case.

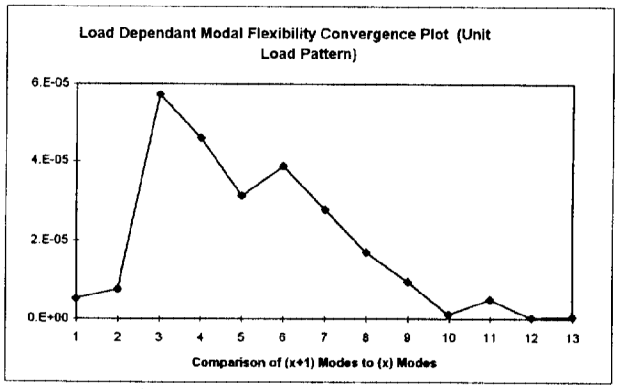

Figure 2 : LMC Plot for Unit Load

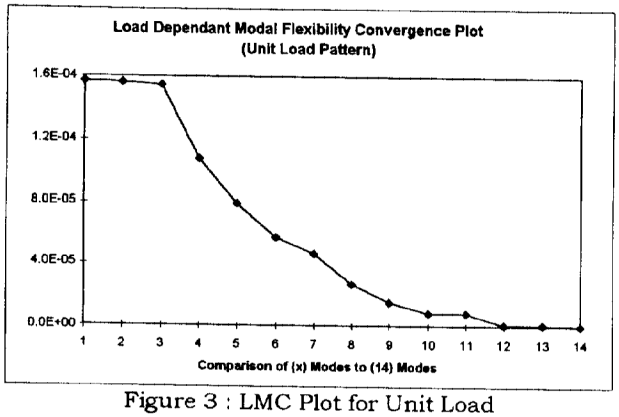

Figure 3 : LMC Plot for Unit Load

In Figure 3, the same procedure is applied; however, the comparison made to m modes included case. Since the differences of the deflected shapes at each measurement degree of freedom for the same modal flexibility matrix itself is zero, the final value in the second figure is zero. The number of modes where each curve begins to converge on zero is an indication of the sufficient number of modes needed in the modal flexibility matrix for that particular loading. Figures 2 and 3 show the modal truncation effect for a uniformly loaded girder. As can be seen, the modal truncation effects decrease considerably within the first 31 Hz where 14 modes are identified for the bearing removal case.

5. COMPARISON OF TWO TESTS--BEFORE AND AFTER DAMAGE

In order to demonstrate and validate the experimental and analytical tools described in this and preceding papers, the test bridge was subjected to different types and levels of damage. The damage scenarios are intended to simulate typical deterioration and damage which may affect the proper functioning and anticipated serviceability and load capacity of steel stringer bridges. Simulations of these damage scenarios have been accomplished in collaboration with ODOT, FHWA, and private consulting engineers. Both before and after damage is induced to the bridge, modal and truck load tests are conducted and the results are evaluated. One of the damage scenarios which will be presented in this paper is the removal of one bearing plate of a girder from one abutment There are six girders total at each abutment. Two tests, one before and one after removal of the bearing plates, were conducted. The results will be analyzed in two spaces: Modal Space and Flexibility Space.

5.1 COMPARISON IN MODAL SPACE

After conducting the two tests, the data from the test bridge is transferred to the UCII lab via modem connection. Post-processing of the data was carried out with X-MODAL software, utilizing the CMIF (Complex Mode Indicator Function) algorithm for preliminary pole location, curve-fitting, scaling, and normalization. Frequency, damping, modal vectors, and the scaling coefficients are obtained. According to the preliminary modal truncation study, at least 10 modes are required to minimize the modal truncation effects. Thirteen modes were extracted from the first 32 Hz bandwidth. In this bandwidth, the data quality was observed to be high and the poles were consistent from test to test. Peaks are selected from the CMIF plot. One important consideration here is to be careful not to pick cross-eigenvalues. Mode tracking is utilized in order to assist in the selection of the valid peaks. Mode tracking is used to determine the range of influence of the modes and detect cross-eigenvalue points. The CMIF plot was decomposed into SDOF modes, which makes it easier to detect correct poles. The CMIF plot and the selected poles are given in Figure 4. In the first 32 Hz band, 13 modes were extracted for the undamaged case.

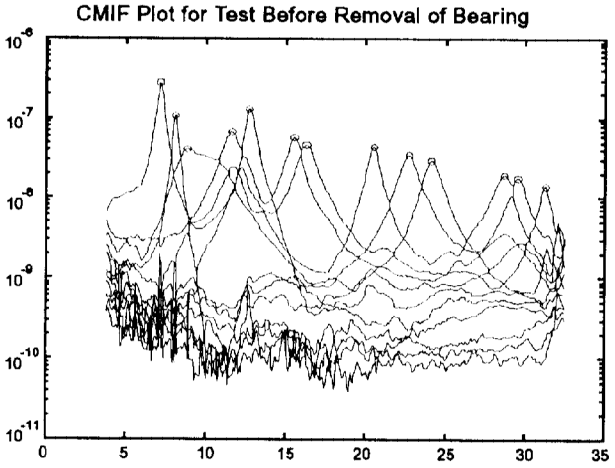

Figure 4 : Complex Mode Indicator Function

After removal of the damage, another impact test was conducted and the data was post-processed in the same manner. From the CMIF plot given in Figure 5, it can be observed that the same modes were identified with an additional local mode around 25 Hz.

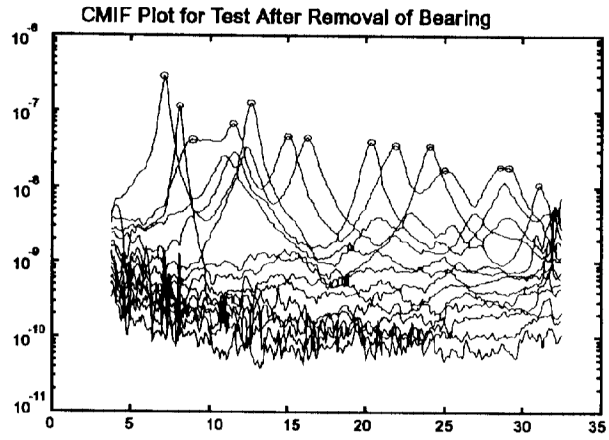

Figure 5 : Complex Mode Indicator Function

The animated shapes of the modes show that local modes in the vicinity of damage are greatly affected by the damage. The additional mode at 24.98 Hz is observed to be a local bending mode in the north span where the damage was induced. The local modes in the north span show some change which lead to low MAC values between these modes before and after damage, whereas the other modes have high MAC values. The list of frequencies and the MAC values before and after damage is given in Table 1.

Table 1: Frequency and MAC Comparison of Two Tests

	Before Removal		After Removal
	8/31/1996 Test		9/10/1996 Test
Mode No.	*Frequency (Hz)*	*MAC*	*Frequency (Hz)*
1	7.13	*0.998*	7.14
2	8.06	*0.997*	8.06
3	8.48	*0.985*	8.52
4	11.55	*0.989*	11.44
5	12.71	*0.993*	12.67
6	15.57	*0.936*	15.12
7	16.27	*0.992*	16.27
8	20.46	*0.998*	20.3
9	22.65	*0.657*	21.92
10	24.06	*0.999*	24.03
11	-	-	24.98
12	28.64	*0.844*	28.52
13	29.48	*0.908*	29.08
14	31.15	*0.981*	30.99

In Figure 6, the local modes affected by the damage can be seen. The bearing is removed from the north end of Girder 3. The mode shape comparison of the two tests from the two inner girders is indicative of the location of the damage.

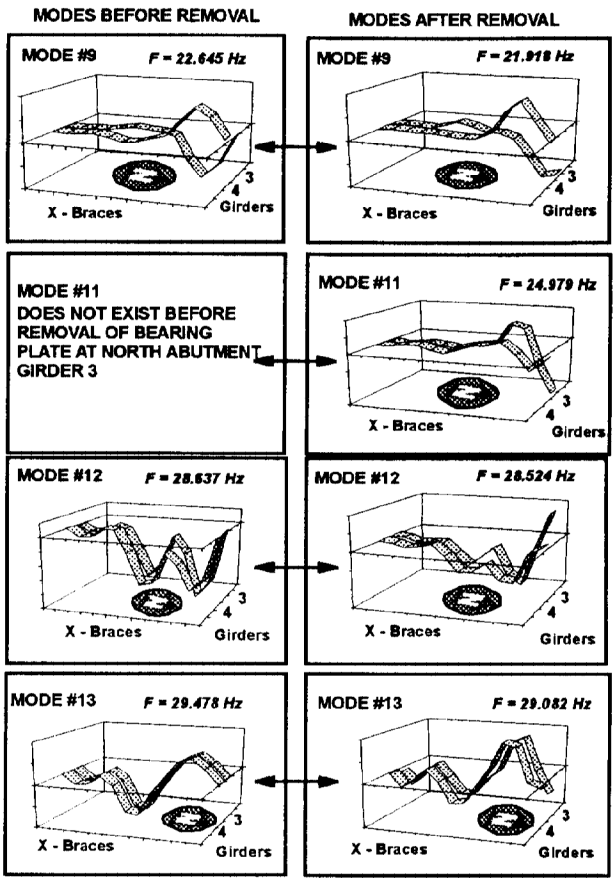

Figure 6 : Mode Shape Comparison

5.2 COMPARISON IN FLEXIBILITY SPACE

Flexibility has been proposed as a reliable signature reflecting the existing condition of bridges. Flexibility also provides a conceptual, quantitative, and damage-sensitive index for condition assessment of bridges. It can also be used to obtain the deflected shapes of a bridge under any loading pattern. The dynamic characteristics of the bridge identified via post-processing the measured FRF's are used to compute the modal flexibility as described in the previous sections.

In order to overcome the non-stationarity due to the environmental conditions, inner and outer girder tests were conducted separately, with 6 common input/output points which were used to splice inner and outer girder tests. Considering the inner girder test itself, the modal flexibility matrix will not include the cross-terms for the unmeasured DOFs. However, a specific load pattern can be utilized that will eliminate this drawback. For this reason, unit loading is defined as loading girders one at a time. This loading pattern is independent of the number of

points measured/tested, as long as the girder under consideration is tested with the same number of points between different tests to be compared. The deflected shape of a particular girder under unit loading defines the condition of the girder. Any discrepancy between the results of different tests is indicative of a change. Figure 7. summarizes the unit loading concept schematically.

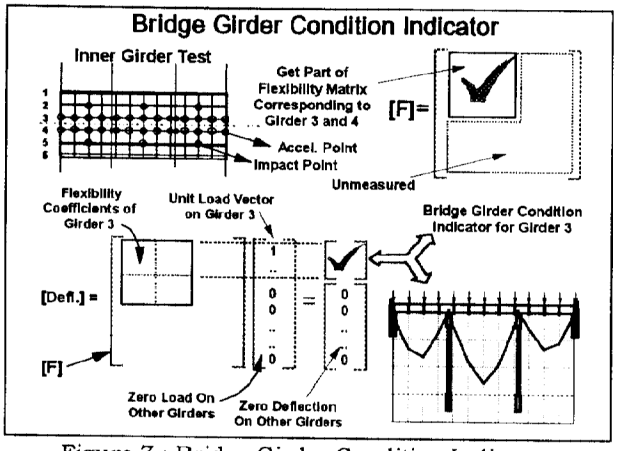

Figure 7 : Bridge Girder Condition Indicator

The before-and-after tests are compared in the same manner. The damage is successfully identified from the after removal test results when compared to the before removal case as shown in Figure 8.

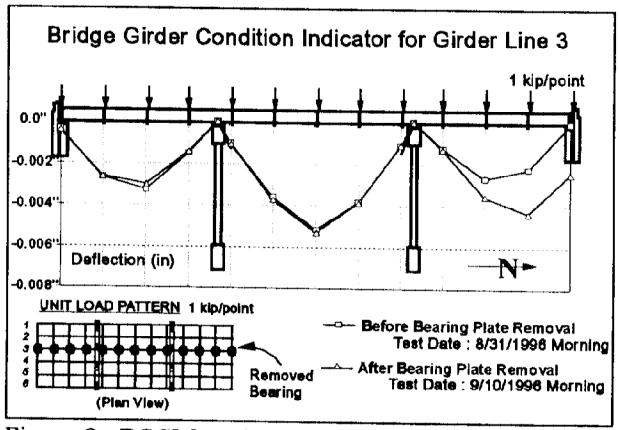

Figure 8 : BGCI for Girder 3 Before and After Damage

The change in stiffness of the bridge is identified with the Bridge Girder Condition Indicator. However, this brings up the question of whether all the major modes are captured, and if the scaling of the modal flexibility is good enough to simulate real load application, how reliable are the results of the modal test? Here, a finite element model (FEM) can be used. The measured modes can be compared to FEM modes. However, calibrated or updated models are not easy to obtain, and in order to calibrate the model, experimental results should be utilized. Another effective way of checking the results of the modal analysis is to conduct diagnostic testing. Diagnostic testing, such as a truck load test, does not provide the state parameters found by modal analysis because of practical limitations associated with these tests. Diagnostic tests, however, are an independent experimental tool which can be used to corroborate the global modal test results. Two diagnostic tests were conducted by instrumenting the bridge with displacement and strain transducers. Two trucks with known wheel loads were positioned in different configurations while the corresponding global displacements and local strains were measured. The tests were conducted both before and after removal of the bearing plate. The truck load data were applied to modal flexibility obtained from modal analysis. The results show very good correlation. The correlation is also an indication that the scaling is correct and the modal truncation effect is not significant. Figures 9 and 10 show the deflection values measured and simulated on the modal flexibility.

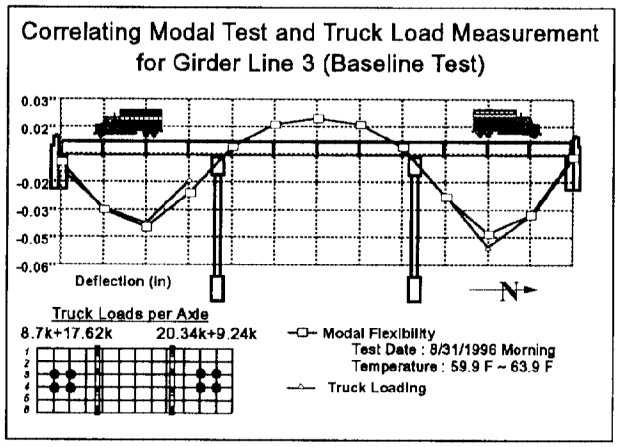

Figure 9 : Truck Load Before Damage

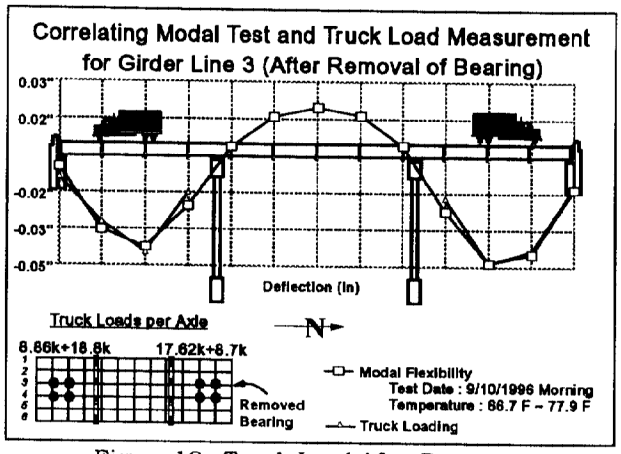

Figure 10 : Truck Load After Damage

6. ANALYSIS OF AFTER REMOVAL DATA AT LOS ALAMOS NATIONAL LABORATORY

The analysis procedure used to process the modal data for the bearing removal case will be described. The modal frequencies, modal damping ratios, and mode shapes were obtained from the data using an Eigensystem Realization Algorithm (ERA)-based curve fitting procedure. A statistical Monte Carlo analysis was also used to verify the quality of the modes by measuring their robustness to realistic levels of noise on the frequency response data. The resulting real modes were mass-normalized so that they were suitable for use in flexibility analysis.

6.1 PRE-CURVE FIT ANALYSIS

The first step in the analysis of the data is to determine the approximate number of modes to be fit. This number is determined using the Multivariate Mode Indicator Function (MIF) [11] and the Complex Mode Indicator Function (CMIF). In this analysis, the CMIF and MIF were computed, and then zoomed to frequency bands of 10 Hz at a time. Approximately 13 modes of significant strength were located between 0 Hz and 40 Hz by inspection of the CMIF and MIF. The approximate frequencies taken from this inspection appear in Table 2, along with which function located them. Most of these modes appeared consistently among the two indicators.

Table 2: Mode Indicator Function

Mode	Est. Freq. (Hz)	Found in MIF?	Found in CMIF?
1	7.2	Y	Y
2	8.1	Y	Y
3	11.6	Y	Y
4	12.4	N	Y
5	12.7	Y	Y
6	15.1	Y	Y
7	16.2	Y	Y
8	20.3	Y	Y
9	21.8	Y	N
10	22.1	N	Y
11	24.1	Y	Y
12	34.6	Y	Y
13	39.7	Y	Y

6.2 MODAL CURVE FITTING

The next step in the analysis is the application of ERA [12]. The ERA procedure is based upon the formation of a Hankel matrix containing the measured discrete-time impulse response data. The shift in this matrix from one time step to the next is then used to estimate a discrete-time state space model for the structure. The next step in the procedure is the determination of the order of the model to compute (i.e., the number of modes in the model). Typically, this method produces many 'computational' modes (i.e., modes which are generated by the curve fit, but which have no physical significance), so it is necessary to overspecify the model order by a large number of modes. The common procedure is to keep the minimum number of singular values needed to accurately reproduce the Hankel matrix. A semilog plot of the singular values of the Hankel matrix, sorted from highest to lowest, is used to determine the minimum number required.

6.3 DISCRIMINATION OF CURVE FIT RESULTS

The model resulting from the ERA analysis had many modes, including computational ones, but it was known from examination of the MIF and CMIF that the data contains only about 13 modes. Thus, it was necessary to apply some discrimination procedures to select the modes that are physically meaningful. There are three indicators developed specifically for use with ERA [13]: Extended Modal Amplitude Coherence (EMAC), Modal Phase Collinearity (MPC), and Consistent Mode Indicator (CMI), which is the product of EMAC and MPC. EMAC is a measure of how accurately a particular mode projects forward (in time) onto the impulse response data. MPC is a measure of the collinearity of the phases of the

components of a particular complex mode. If the phases are perfectly linear (i.e., either in phase or 180 degrees out of phase with each other), this mode is exactly proportionately damped, and can then be completely represented by a corresponding real mode shape. Thus, EMAC is a temporal quality measure, and MPC is a spatial quality measure. Typically, it is reasonable to start with values of EMAC = 0.7, MPC = 0.7, and CMI = 0.5, and then see if all of the modes of interest (as determined by MIF and CMIF inspection) are preserved. In the current study, all of the 13 modes of interest passed this criteria, including all of the modes below 20 Hz, so these values of EMAC, MPC, and CMI were used as the cutoff values. Visual inspection of the mode shapes was conducted for the extracted modes. Modal assurance criterion (MAC) is another useful tool for discriminating modes. The synthesis of the FRF using the identified modes and overlay onto the data can also be a somewhat useful tool for determining the accuracy of the modal curve fit. In the current case, the identified modal set provided fairly accurate overlays onto the measured FRF's.

6.4 POST-CURVE FIT ANALYSIS

Once the basic ERA parameters had been determined such that the modes of interest were identified and passed the discrimination criteria, a Monte Carlo analysis was performed to measure the statistical confidence in the results of the identification. Using the measured Coherence function, 1 standard deviation uncertainty bounds were computed on the FRF magnitude and phase using the formulas derived by Bendat and Piersol [14]. These bounds represent the estimated random variations on the FRF resulting from the measured level of random noise in the measurements according to the Coherence function. These confidence bounds on the FRF were propagated through the identification procedure using a Monte Carlo analysis. The procedure is summarized as:

1) Add Gaussian random noise to the FRF's using the noise standard deviations computed from the Coherence function. This additional noise represents a realistic level of random variations in the measurements.

2) Run the noisy FRF through the ERA identification procedure and apply the modal discrimination using the previously computed parameters.

3) Compute the mean and standard deviation of each modal frequency, damping ratio, and mode shape component over the total number of runs.

4) Repeat steps 1, 2, and 3 until the means and standard deviations in step 3 converge.

For the current study, the convergence took about 30 runs. This convergence determines the sufficient sample size to provide significant confidence in the statistical estimates.

The statistics computed on the test bridge data are shown in Table 3. The first column contains the mode number. The second column is the mean of the identified modal frequency in Hertz. The third column contains the standard deviation of the modal frequency in Hertz (absolute deviation), and the fourth column contains the standard deviation of the modal frequency as a percentage of the mean (relative deviation). The fifth column is the mean of the identified modal damping ratio. The sixth column contains the standard deviation of the modal damping ratio (absolute deviation), and the seventh column contains the standard deviation of the modal damping ratio as a percentage of the mean (relative deviation). None of the modes show a significant error in modal frequency. Modes 3, 9, and 10 show a significant error in modal damping ratio. None of these errors were large enough to exclude the mode from the identified modal set. However, the error in modal damping ratio should be considered when performing analyses that use these values (e.g., time history prediction or FRF synthesis). Also, recalling that modes 9 and 10 were found inconsistently between the indicator functions and have a significant amount of spatial similarity as indicated by the MAC, it is not surprising that they demonstrate a significant amount of statistical uncertainty as well. It is possible that these modes are poorly excited or that they are spectrally close to a 'tuned absorber'. An absorber is a local vibration that can cause the data to appear as though two separate modes are in close spectral proximity. The spatially similar mode shapes support this hypothesis, assuming that the location of the tuned absorber does not coincide with one of the sensor locations. These modes are kept in the set, however, as a result of their high values of EMAC and MPC.

Table 3 : Statistical Analysis

Mode	Freq. (Hz)	1 STD (Freq)	1 STD Freq (%)	Damp Ratio	1 STD Damp	1 STD Damp (%)
1	7.193	4.890E-04	0.007	3.372E-2	8.461E-5	0.251
2	8.122	7.518E-04	0.009	2.483E-2	6.762E-5	0.272
3	11.615	6.446E-03	0.055	5.248E-2	4.411E-3	8.404
4	12.435	4.734E-03	0.038	5.305E-2	2.908E-4	0.548
5	12.702	2.576E-03	0.020	2.564E-2	2.729E-4	1.064
6	15.090	5.406E-03	0.036	4.038E-2	2.780E-4	0.688
7	16.233	7.164E-03	0.044	3.978E-2	5.063E-4	1.278
8	20.305	3.689E-03	0.018	2.550E-2	1.969E-4	0.760
9	21.807	1.604E-01	0.736	4.193E-2	9.099E-3	21.702
10	22.078	6.267E-02	0.284	3.264E-2	2.266E-3	7.003
11	24.075	2.529E-03	0.011	2.617E-2	1.579E-4	0.603
12	34.550	1.984E-02	0.057	1.674E-2	5.542E-4	3.311
13	39.742	2.636E-02	0.066	1.980E-2	7.545E-4	3.810

Next, the results of the modal analyses conducted at the University of Cincinnati Infrastructure Institute and Los Alamos National Laboratory are compared. Table 4 presents the identified modes from these two different studies and the MAC values between them.

Table 4 : Frequency and MAC Comparison of UCII and LANL Results

	UCII Results		LANL Results
	After Removal		After Removal
	9/10/1996 Test		9/10/1996 Test
No.	Frequency (Hz)	MAC	Frequency (Hz)
1	7.14	0.999	7.193
2	8.06	0.999	8.121
3	8.52	-	-
4	11.44	0.985	11.618
5	-	-	12.433
6	12.67	0.999	12.702
7	15.12	0.962	15.091
8	16.27	0.999	16.229
9	20.3	0.872	20.307
10	-	-	21.794
11	21.92	0.944	22.113
12	24.03	0.977	24.076
13	24.98	-	-
14	28.52	-	-
15	29.08	-	-
16	30.99	-	-
17	-	-	34.55
18	-	-	39.746

As can be seen from the table, the results show differences especially after the 25 Hz range. This may be due to differences in the way the modal identification computations were conducted. The modal flexibilities also show some inconsistencies as a result of the missing modes in two sets. Since the analysis at LANL was conducted immediately before this paper was prepared, the differences between the two result sets will be further investigated and presented during the conference.

7. CONCLUSIONS

Complex Mode Indicator Function is used as the parameter estimation algorithm in the analysis of the experimental data of the test bridge. CMIF is compatible with the concept of Multiple Reference Impact Testing. Compared to the sophisticated commercial algorithms, it minimizes the user interaction and results are not greatly disturbed with the shifts of the poles of the structure due to non-stationarity caused by environmental effects. Results obtained from the CMIF algorithm correlate with the static truck load test measured with displacement transducers.

The results provided from the Los Alamos National Laboratory researchers correlate reasonably well with the UCII results in the first 24 Hz range. The data is post-processed using the Eigensystem Realization algorithm. It should be considered that type of condensation used to reduce the data to match the number of unknowns for an over-specified problem like this might change the results. Therefore, there is no unique answer to the problem. However, the *best* answer can be sought depending on the objective of the research. The correlation study will be conducted rigorously between the two institutions in future corroborations to get the *best* possible answer for the future damage scenarios.

The quality control of the post-processed results should be checked both in modal and flexibility space. Any computational modes or problems in scaling can be observed when the modal analysis results are transformed to flexibility space. Therefore, modal flexibility derived from the experimental data is also used to verify the physical completeness of the results.

Modal flexibility can be derived directly from the Frequency Response Functions. This derivation does not require unit-mass normalized modal vectors. In order to get a close approximation of the flexibility matrix, the modal truncation effects should be minimized. Modal truncation on the flexibility is also a function of load. Depending on the loading condition, the required number of modes for a good approximation may change. A new index is utilized for Load Dependent Flexibility Convergence.

Comparisons are made of two data sets. Significant differences in the mode shapes are observed. After removal of one bearing plate, a local mode which does not occur at the before removal case is observed. Global modes of the bridge are not affected when the MAC values are considered. Local modes in the vicinity of damage are affected most. Frequency change between the before and after tests are slim and not indicative of the damage.

In order to preclude the non-stationarity in the data set, tests are designed to be conducted within a short period of time. However, these tests do not yield the cross-terms between the measured and unmeasured DOF's. A specific load pattern is utilized by loading each girder one at a time. This loading suppresses the contribution of unmeasured deflection coefficients. The resulting deflections are named as Bridge Girder

Condition Indicator. The difference in BGCI's between two tests before and after removal of the bearing plate located the damage. In addition, quantification of the damage is made successfully for a static truck load test. The two static truck load test results also correlate with the modal analysis results.

8. ACKNOWLEDGMENTS

A peer review panel has been formed for the current project: Drs. Brown, SDRL, University of Cincinnati; Cantieni, EMPA, Switzerland; Ewins, Imperial College, UK; Farrar, Los Alamos National Labs; Rubin, Aerospace Corporation; and Yao, Texas A&M. Their recent workshop, invaluable advice, and future collaboration have brought international recognition to this research and assured the successful attainment of the project goals.

This research is supported by the Ohio Department of Transportation, Research and Development, and the FHWA through the HPR Program. Mr. Edwards, Hanhilammi, Barnhart, Welker, and Eltzroth of ODOT and Mr. Shamis of Ohio FHWA have extended their confidence and support for which we are grateful. We also acknowledge the valuable input provided by Dr. Chase of FHWA Headquarters and the Office of Research at Washington, D.C.

9. REFERENCES

[1] Ewins, D.J., "Modal Testing : Theory and Practice", John Wiley and Sons, Inc., 1984.

[2] Hogue, T.D. and Aktan, A.E., "Localized Identification of Constructed Facilities", J. of Structural Engineering, 117,23 (1), 1991.

[3] Raghavendrachar, M. and Aktan, A.E., "Flexibility for Multireference Impact Testing for Bridge Diagnostics', J. of Struct. Eng. ASCE 118(8), 1992.

[4] M.Lenett, F.N. Catbas, V.Hunt, A.E. Aktan, A. Helmicki and D.L. Brown, "Issues In Multi-Reference Impact Testing of Steel Stringer Bridges", Proceedings of the Fifteenth International Modal Analysis Conference, 1996.

[5] W.A. Fladung, "The Development and Implementation of Multiple Reference Impact Testing", Masters Thesis, University of Cincinnati, 1994.

[6] Shih, C.Y., Tsuei, Y.G., Allemang, R.J., Brown, D.L., "Complex Mode Indicator Function and Its Application to Spatial Domain Parameter Estimation," Proceedings of the Seventh International Modal Analysis Conference, 1989.

[7] Shih, C.Y., Tsuei, Y.G., Allemang, R.J., Brown, D.L. "Frequency Domain Global Parameter Estimation Method for Multiple Reference Frequency Response Measurements", Mechanical Systems and Signal Processing, Vol.2, No.4, 1988.

[8] Leurs, W., "Modal Parameter Estimation Based on the Complex Mode Indicator Functions", Proceedings of the Eleventh International Modal Analysis Conference, 1993.

[9] Fladung, W.A., Phillips, A.W., Brown, D.L. " Specialized Parameter Estimation Algorithms for Multiple Reference Testing",Proceedings of the Fifteenth International Modal Analysis Conference, 1996.

[10] X-MODAL, Structural Dynamics Research Laboratory, University of Cincinnati, 1993.

[11] Allemang, R.J., "Vibrations: Experimental Modal Analysis," University of Cincinnati Class Notes, UC-SDRL-CN-20-263-663/664.

[12] Juang, J.N. and Pappa, R.S., "An Eigensystem Realization Algorithm for Modal Parameter Identification and Model Reduction," Journal of Guidance, Control and Dynamics, Vol. 8, No. 5, Sept.-Oct. 1985, pp. 620-627.

[13] Pappa, R.S., Elliott, K.B., and Schenk, A., "Consistent-Mode Indicator for the Eigensystem Realization Algorithm," Journal of Guidance, Control and Dynamics, Vol. 16, No. 5, Sept.-Oct. 1993, pp. 852-858.

[14] Bendat, J.S. and Piersol, A.G., Engineering Applications of Correlation and Spectral Analysis, John Wiley and Sons, New York, 1980, p. 274.